2017

Analysing the risks of storing strong waste brine in a deep saline aquifer with particular reference to Potasio Rio Colorado mine in Argentina

Abukhlif, A.

Abukhlif, A. (2017) 'Analysing the risks of storing strong waste brine in a deep saline aquifer with particular reference to Potasio Rio Colorado mine in Argentina', The Plymouth Student Scientist, 10(1), p. 64-101.
http://hdl.handle.net/10026.1/14140

The Plymouth Student Scientist
University of Plymouth

Analysing the risks of storing strong waste brine in a deep saline aquifer with particular reference to Potasio Rio Colorado mine in Argentina

Arkan Abukhlif

Project Advisor: Daniel Hatton, School of Engineering, Faculty of Science and Engineering, University of Plymouth

Abstract

Potasio Rio Colorado is a potash development project located in the Mendoza Province of Argentina that produces the majority of potassium used for agricultural fertilisers. The potassium is extracted through mining underground water-soluble minerals such as potash by dissolving the minerals with water; this process is called solution mining. A common waste product of solution mining that needs to be disposed of to improve the prospects of waste disposal in order to help solve a major societal problem "groundwater contamination" is strong aqueous solution, referred to as brine. This report assesses the risks associated with storing brine in a deep saline cylindrical aquifer in the following way:

- Can strong brine be stored in a deep saline aquifer without leaking back to the surface?
- Will the published injection rates of brine result in hydraulic fracturing leading to additional paths for brine to leak back to the surface?

The Carter-Tracy technique was used to determine the cumulative water influx within the aquifer which gave insight to determining the possibility of brine outcropping using Darcy's radial flow for incompressible fluids. The applicability of the Carter-Tracy technique was maximised by limiting the time-steps used to less than 30 days. The results obtained were evident enough to prove brine not only outcrops at high rates (lowest: 356 m^3/day, highest: 2395 m^3/day) but also the high injection rates set by Vale will cause the rock to fracture leading to additional paths for brine to leak towards the surface. The applicability of this method has been validated with a set of results that has previously been published in a peer-reviewed journal.

The conclusion drawn was based on the stratigraphic diagram of the permeable and impermeable layer provided by Legarreta (1985) and did not give a clear indication that the surface treated as the surface in the calculations was the actual ground-surface, leaving some uncertainty. Recommendations for further research have been pointed out, but these solutions offered for the prevention of groundwater salinisation should not be implemented until one of these approaches has been assessed, found effective, and deployed.

Contents

List of Figures

List of Tables

List of Equations

Nomenclature

Symbol	Definition
h	Aquifer Thickness
g	Acceleration due to gravity
A	Cross-sectional area through which the water flows
$n(n-1)$	Current, previous, time step
P_r	Density of rock
$P`_D$	Derivative of dimensionless pressure with respect to dimensionless time
t_D	Dimensionless time
P_D	Dimensionless pressure
μ	Dynamic viscosity
f	Encroachment angle
E_i	Exponential integral
K	Hydraulic Conductivity
∇h	Hydraulic Gradient

P_i	Initial pressure
L	Length
P_w	Maximum calculated pressure
Pe	Peclet number
κ	Permeability
Φ	Porosity
Pr	Prandtl number
r_e	Radius of the aquifer
Re	Reynolds number
C_f	Rock formation compressibility
q	Specific Discharge, Darcy's velocity
S_S	Specific Storage
S	Storativity
T	Temperature of underground brine solution
D_H	Thermal diffusivity
Δp_n	Total pressure drop
C_t	Total reservoir compressibility
B	Van Everdingen-Hurst water influx constant
Q	Volume of water passing per unit time
J_Z	Volume of fluid passing
r_w	Wellbore radius

Terminologies

(Duffield, 2015) Except where they have been individually referenced.

Aquifer: A layer of sediment or rocks capable of conveying significant amounts of water.

Aquifer Diffusivity (α): The ratio of transmissivity to storativity. $\alpha = \mathrm{T}/S$

Aquifer Thickness (b): Is the vertical thickness of an aquifer where the pore spaces are saturated with water.

Aquitard: A layer of sediment or rock that transmits small quantities of water when compared to an aquifers.

Brine: Is strong aqueous solution of salt (usually sodium chloride) in water.

Confined Aquifer: An aquifer confined between aquitards.

Consolidated rocks: Is a rock made from materials that have been cemented together such as sandstone and limestone.

Darcy's velocity (q): Flow rate per unit cross-sectional area of the aquifer.

Diffusive transport: Pressure propagation in the elastic aquifer.

Displacement (H): Change in water level measured from a static position.

Hydraulic Conductivity (K): Constant of proportionality defining the specific discharge of a porous medium under a unit hydraulic gradient.

Hydraulic Gradient (∇h): Hydraulic head loss per unit distance in the direction of the flow (Bengtson, 2011).

Lithostatic Gradient: Difference in pressure between top and bottom layers of rock.

Peclet number (P_e): A dimensionless number expressing the ratio of advective to dispersive transport rates.

Permeability (κ): Is measure of the ability of a porous material to allow fluids to pass through it.

Porosity (ϕ): Ratio of void volume to the total volume of an unconsolidated material.

Reynolds number (Re): A dimensionless number expressing the ratio of inertial to viscous forces.

Specific Storage (S_S): Volume of water realised from storage from a unit volume of aquifer per unit decline in hydraulic head.

Storativity (S): Volume of released water from a confined aquifer per unit surface area per unit decline in hydraulic head normal to the surface of a confined aquifer.

Superposition concept: Breaks the position dependence down to individual locations, thus making it easier for humans to understand (Shankar, 2008).

Sylvinite: Mixture of minerals that include potassium chloride and sodium chloride (Anderle et al., 1979).

Transmissivity (T): The product of hydraulic conductivity and saturated thickness.

Unconfined Aquifer: An aquifer in which water table forms its upper boundary.

Unconsolidated rocks: Rocks made from loose materials such as clay, sand, and gravel.

Water Table: The surface of a porous medium on which the fluid pressure is equal to atmospheric pressure due to the fact that the exerted hydraulic head is zero (Bengtson, 2011).

Project Aims and Objectives

Aims

- Improving the prospects of safe disposal of strong waste brine caused by important engineering projects to help solve a major societal problem (groundwater contamination).

Objectives

- Emphasis the growing threat of groundwater salinisation and liquid hazardous wastes.
- Carry out documentary research on groundwater hydrology.
- Complete documentary research on fluid storage and diffusive transport.
- Execute a documentary study on fluid transport and motion in porous media.
- Check whether hydraulic fracturing occurs in the region of study to ensure the safety of storing brine in a deep saline aquifer.
- Define the Cartier-Tracy method and its assumptions as it is the appropriate method for predicting whether the lithostatic pressure is high enough to cause hydro-fracturing.
- Determine the water influx using the Carter-Tracy technique to help improve prospects of waste disposal.
- Describe the physics behind groundwater storage.
- Determine whether strong waste brine could be stored in a deep saline aquifer with particular reference to Potasio Rio Colorado mine in Argentina to help improve the prospects of waste disposal.
- Conclude whether the stored brine within the aquifer would outcrop leading to contamination issues.

Introduction

With an investment of 5.9 billion US dollars, Vale's mineral fertilisers project Rio Colorado Potassium is the biggest as of now in Argentina; not only in terms of the investment, but also in terms of establishment's size as it stretches crosswise over five provinces, from Mendoza to Bahia Blanca (Kiernan, 2013). Throughout the project's initial stages, it is predicted to produce around 2.1 to 2.3 million tonnes of potassium chloride a year, growing to almost 4.3 million tonnes a year by 2018 (Pearson, 2013).

In this project, the main use of potassium chloride is for agricultural fertilisers. Potassium chloride represents the vast majority of potassium utilised in global agriculture as it accounts for almost 96% of the world's potash capacity (Garrett, 1996).

Solution mining is a process whereby valuable deep-underground resources which are (or can be made to be) soluble in water are extracted by injecting water into a borehole, and sucking the resulting aqueous solution of the valuable product (potassium chloride) either out of the same borehole, or out of another nearby borehole (Yazicigil et al., 2009).

A common waste product of solution mining, which needs to be disposed of to help reduce groundwater contamination, is a strong aqueous solution of sodium chloride usually referred to as brine (Schreck, 1998).

The potassium chloride is contained in a deposit of sylvinite which is located in a region of roughly 80000 hectares ($8x10^8$ m^2) in the division of Mendoza, at a depth of around 1000 to 1200 metres (Els, 2013). The ore will be extracted by a dissolution process as shown in Figure 1. Two wells will be drilled into the deposit through which high-temperature water is injected to dissolve the ore. The potassium rich brine will then be extracted through another pipe and pumped to the processing plant in the tanks area (Pearson, 2013).

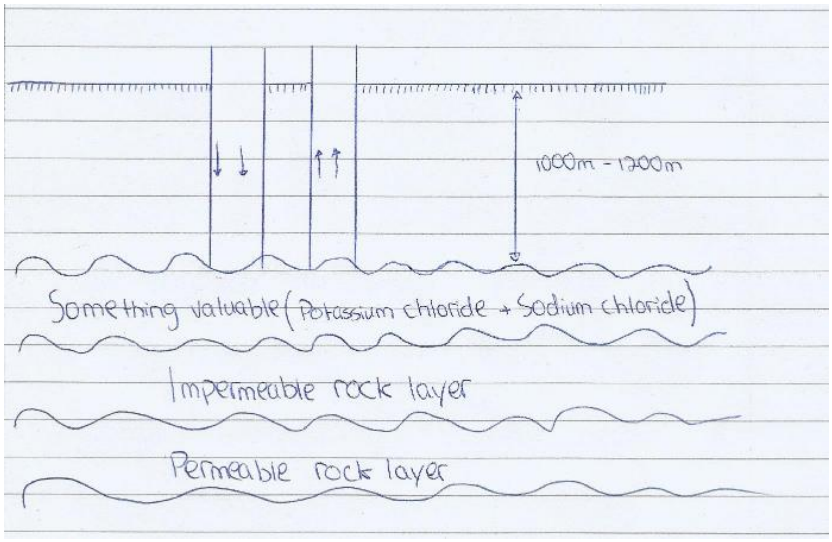

***Figure 1**: Sketch of dissolution process by which the ore is extracted.*

The operation utilises water extricated from the adjacent Colorado River in agreement with the capture level approved by Mendoza's provincial legislature. From the tanks, the saline solution (brine) will be separated into two salts: sodium chloride and potassium chloride. A key part of the rationale for this project is the disposal of strong waste NaCl brine in a deep saline aquifer to help solve a major social problem "groundwater contamination".

The potassium chloride then proceeds to a drying plant where the humidity (moisture) is removed, and the sodium chloride solution (strong waste brine) is then deposited in specially built installations found 18 kilometres from Rio Colorado (Kiernan, 2013).

The growing threat of groundwater salinisation and irrigation-induced soil salination is becoming an important issue in hydrology, agronomy, and soil sciences (Valipour, 2014). For instance, more than one-third of the world's irrigated land is affected by soil salinisation and this condition poses a threat to environmental conservation and food security (Singh, 2015).

Hazardous wastes are a result of household, economic and mining activities which could lead to a substantial impact on the environment and our health if not managed and disposed of safely (Carter, 2011).

Among the waste produced within the EU in 2012, around 100 million tonnes (4% of the total waste) were classified as hazardous liquid waste which is equivalent to approximately 198 kilogrammes of hazardous waste per EU resident as shown in Table 1 (Ec.europa.eu, 2015).

	Total waste generation		Hazardous waste		Haz. Waste share of total waste generation
	2010	2012	2010	2012	2012
EU-28	2 460 330	2 514 220	97 490	99 850	4%
Belgium	62 537	67 630	4 479	4 258	6%
Bulgaria	167 396	161 252	13 553	13 407	8%
Czech Republic	23 758	23 171	1 363	1 481	6%
Denmark	16 218	16 332	1 225	1 193	7%
Germany	363 545	368 022	19 931	21 984	6%
Estonia	19 000	21 992	8 962	9 159	42%
Ireland	19 808	13 421	1 972	1 385	10%
Greece	70 433	72 328	292	297	0%
Spain	137 519	118 562	2 991	3 114	3%
France	355 081	344 732	11 538	11 303	3%
Croatia	3 158	3 379	73	123	4%
Italy	158 628	162 765	8 543	9 474	6%
Cyprus	2 373	2 086	37	31	1%
Latvia	1 498	2 310	68	95	4%
Lithuania	5 578	5 679	105	137	2%
Luxembourg	10 441	8 397	380	315	4%
Hungary	16 735	16 310	541	700	4%
Malta	1 353	1 452	25	29	2%
Netherlands	120 384	123 613	4 485	4 860	4%
Austria	34 883	34 047	1 473	1 066	3%
Poland	159 458	163 378	1 492	1 737	1%
Portugal	17 313	14 184	667	545	4%
Romania	219 310	266 976	666	671	0%
Slovenia	5 986	4 547	117	133	3%
Slovakia	9 384	8 425	415	370	4%
Finland	104 337	91 824	2 559	1 654	2%
Sweden	117 645	156 307	2 528	2 697	2%
United Kingdom	236 568	241 101	7 004	7 631	3%
Iceland	511	529	8	16	3%
Liechtenstein	312	467	8	4	1%
Norway	9 433	10 721	1 763	1 357	13%
Montenegro	:	386	:	3	1%
FYR of Macedonia	2 328	8 472	150	679	8%
Serbia	33 616	55 003	11 161	14 457	26%
Turkey	783 423	1 013 226	3 226	3 988	0%
Bosnia and Herzego	:	4 457	:	946	21%
Kosovo	:	1 167	:	1	0%

Table 1: Hazardous liquid waste generated in Europe between 2010 and 2012. Reproduced from (Ec.europa.eu, 2015).

Between 2004 and 2012, the EU experienced a 10% increase in hazardous liquid waste generated per inhabitant as shown in Figure 2 (Ec.europa.eu, 2015).

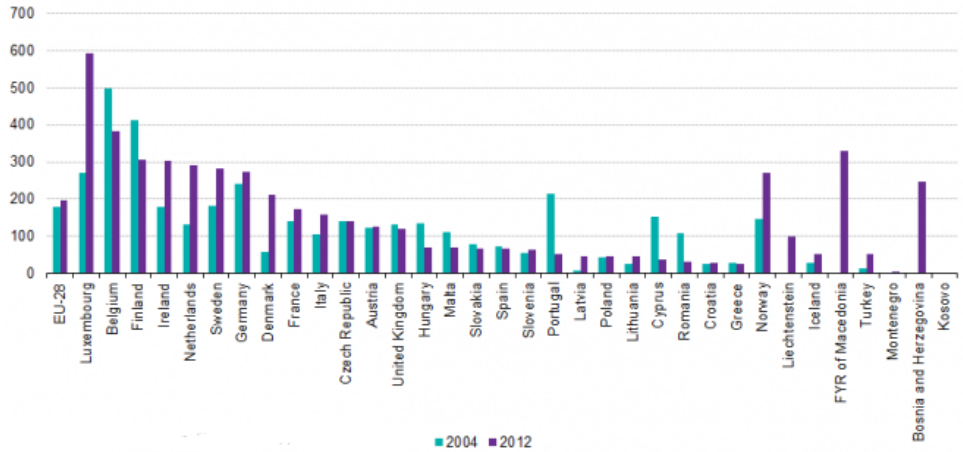

Figure 2: Hazardous liquid waste generated between 2004 and 2012. Reproduced from (Ec.europa.eu, 2015).

Improving the prospects of safe disposal of waste brine

The selection of a disposal method for strong waste brines that allows money-making mining activities to continue while minimising the environmental harm associated with

contamination of farmland with those brines raises the following need for an environmental safety case for this underground disposal method:

- Can strong waste brine be stored in a deep saline aquifer with particular reference to Potasio Rio Colorado mine in Argentina?
- Would the stored brine within the aquifer outcrop causing brine to reach the surface at an outcrop?

The reason these objectives are of genuine importance is due to the significant impact they might result in, for instance, if brine outcrops and reaches the surface then highly saline water would contaminate agricultural lands and rivers (Fetter, 2001). Furthermore, the additional pressure associated with the injection of brine may fracture the aquitard, impermeable layer overlying the aquifer, creating additional pathways for the brine to leak back to the surface (Birkholzer et al., 2013).

The use of evaporative ponds in desalination plants was considered as an alternative method for the disposal of strong waste brine (Ahmed et al., 2000). However, this approach was not perfectly satisfactory in every case because in the event of windy days brine might migrate to agricultural lands causing contamination issues.

Literature Review

Documentary research on groundwater hydrology

Groundwater hydrology is the study of water in porous materials such as sandstone/limestone. Groundwater refers to the water, in the saturated zone, below the water table at which the water moves freely into the wells under pressures higher than that of atmospheric pressure (Suckow, 2014). In 1856, Henry Darcy developed an equation that defines the flow of groundwater in a porous medium which helps predict the rate of flow through a geologic media, aquifer (Anderson, 2007):

$$\mathrm{q} = Q/A = -\mathrm{K}\,\nabla\mathrm{h}$$

Equation 1: Henry Darcy's law. Reproduced from (Anderson, 2007).

where,

q is Darcy's velocity.

Q is the volume of water passing per unit time.

A is the cross-sectional area through which the water flows

K is the hydraulic conductivity of the aquifer.

$\nabla\mathrm{h}$ is the hydraulic gradient.

Three important aspects can be noticed from examination of Bear and Verruijt's (1987) illustration of flow through an inclined sand column, where Q is the flow rate (Masoodi and Pillai, 2010):

- Q is proportional to head difference.
- Q is proportional to the cross-sectional area of an aquifer.
- Q is inversely proportional to length. As length increases, the flow rate decreases.

$$Q \propto \mathrm{A}\,\frac{\mathrm{h}_2 - \mathrm{h}_1}{L}$$

Equation 2: Darcy's law multiplied by area. Reproduced from (Masoodi and Pillai, 2010).

Fluids move along grain boundaries or fractures. The rate in which a fluid is transported is governed by the geometry of the channel network, the viscosity of the fluid, and the pressure differential causing the flow (Philpotts and Ague, 2009). The flow velocity is proportional to the square of the channel width (w). If the flow occurs along planes with a width larger than w^2, the flow rate drastically increases as a result (Philips, 1991).

The permeability depends solely on the properties of the matrix and is directly related to the average size and abundance of the through-going channels (Stiles, 1924). Permeability and porosity differ in the order of magnitude from one rock layer to the other and should be taken from experimental literature as shown in Table 2 and Table 3 (Tiab and Donaldson, 2015; Speight, 2014).

Rock type		Permeability (m^2)
Consolidated rocks	Sandstone	$10^{-13} \rightarrow 10^{-17}$
	Limestone and dolomite	$10^{-13} \rightarrow 10^{-16}$
	Shale	$10^{-16} \rightarrow 10^{-20}$
Unconsolidated rocks	Gravel	$10^{-7} \rightarrow 10^{-10}$
	Clean sand	$10^{-9} \rightarrow 10^{-13}$
	Silt sand	$10^{-10} \rightarrow 10^{-14}$

Table 2: Permeability of different types of rocks. Reproduced from (Qiao and Li, 2014).

Rock type		Range of Porosity (%)
Consolidated rocks	Sandstone	0.05 → 0.3
	Limestone and dolomite	0 → 0.2
	Shale	0→ 0.1
Unconsolidated rocks	Gravel	0.2 → 0.4
	Clean sand	0.2 → 0.5
	Silt sand	0.3 → 0.7

Table 3: Porosity of different types of rocks. Reproduced from (Nonner, 2015).

Fluid storage

Work cited in this report is incomplete due to not taking into account the storage effects associated with the elasticity of the rock material.

Water stored in soil can be divided into three categories (Croney and Coleman, 1948):

- Gravitational water.
- Groundwater.
- Held water.

Gravitational water enters the soil at the surface and travels in the direction of gravity until it reaches an impermeable layer. Once it reached the impermeable layer, gravitational water builds up to a level known as the water table. Water below that level, water table, is referred to as groundwater. Held water is a result of the water stored in the pores of the soil due to the surface tension forces (Osman, 2013).

Groundwater is stored in reservoirs referred to as aquifers. As stated by Philips (1991), an aquifer is a porous and permeable media that is composed of a network of small areas of

cracks where sediment grains are not perfectly aligned. These areas which are a result of cracks, create spaces within the sediments or rocks to allow the fluid to move.

In other words, an aquifer is a geological formation which contains water and allows significant amounts of water to flow through it under normal felid condition (Bear and Verruijt, 1987). Todd (1959) traced the term aquifer to its Latin origin: aqui comes from aqua, meaning water, and fer from ferre, to bear. The more porous an aquifer is, the higher the connectivity between the pore spaces, the greater the flow velocity is.

An aquifer is surrounded by a highly impermeable layer referred to as aquitard which prevents the fluid stored within from outcropping or leaking back to the surface.

An aquifer can be classified into two categories: confined and unconfined aquifers (Bear and Verruijt, 1987). A confined aquifer is bounded vertically by a relatively impermeable rock layer (aquitard). An unconfined aquifer implies the presence of water table, allowing the fluid to flow into and out of the aquifer. In this framework, outcropping is described as the process of water leaving the aquifer through its intersection with the ground-surface (Price, 2013).

In reservoir engineering, there are more uncertainties attached to this subject (non-uniform permeability and porosity) than any other (Donnez, 2012); and the reason for this was simply because not enough wells are drilled into the aquifer to get the necessary information about (Satter et al., 2008):

- The geometry of the aquifer,
- Porosity,
- Permeability,
- Fluid properties.

Instead, these properties have to be determined from what has been observed in the reservoir.

The voids in the soil do not behave like reservoirs in which the water can be stored, but instead, they are tiny irregular pathways which water can flow through. In this framework, there are storativity effects due to the elastic deformation of the rock as pressure increases this allowing the accumulation term to be none zero (Phillips, 2009). The concept of storativity in a confined and unconfined aquifer is illustrated by Zhang (2014).

Diffusive transport

A material has two basic means of transport:

- Advection
- Diffusion

Diffusion happens when an atom moves independently to its surrounding in response to the force developed by the potential gradient (Bennett, 2012; Logan, 1999). Advection occurs when an atom behaves passively, being moved only when surroundings move (Kresic, 2006). For instance, ions carried in solution by a fluid that flows through a rock would be an example of advection whereas diffusion of an ion down a concentration gradient within a solution would be the case of diffusion (Healy and Scanlon, 2010; Charbeneau, 2006).

Both means of transport play a significant role in transport; however, their rates greatly differ thus capable of acting over different distances within the given timescale (Phillips, 2009).

Column experiments showed that as the specific discharge increases, the relation between the specific discharge and the hydraulic gradient gradually varies from the linear

relationship, expressed in Darcy's law (Bear and Verruijt, 1987). It is important to note that Darcy's law is valid as long as the Reynolds number does not exceed values ranging between one and ten as most groundwater flow occurs within this range (Bear and Verruijt, 1987).

As the Buoyancy number and Peclet number increase, the velocity decreases as a result (Park et al., 2009). Brine reduces the upward vertical velocity when both the gravitational forces dominate the inertial forces (high Buoyancy number) and when the transport is advection dominated (large Peclet number).

In this framework, the Reynolds number is small, yet the Peclet number is extremely high validating that advection would be of more relevance to us, and this is possible because the kinematic viscosity is much larger than thermal diffusivity. In other words, when the thermal conductivity is low, it yields a small thermal diffusivity as characterised by Equation 3; and since the dynamic viscosity is high, it results in a high Prandtl number and low Reynolds number to satisfy Darcy's law as characterised by Equation 4. Since the kinematic viscosity is much greater than the thermal diffusivity, it results in a high Peclet number.

$$D_H = \frac{k}{\rho * C_p}$$

Equation 3: Thermal diffusivity. Reproduced from (Theodore, 2011).

where,

D_H is the thermal diffusivity.

k is the thermal conductivity.

$$Peclet\ number = Reynolds\ number * Prandtl\ number = \frac{\rho * u * L}{\mu} * \frac{\mu}{\rho * D_H} = \frac{u * L}{D_H}$$

Equation 4: Peclet number as a function of Reynolds and Prandtl number. Reproduced from (Theodore, 2011).

where,

ρ is the density.

u is the velocity.

L is the characteristic length.

μ is the dynamic viscosity.

Fluid transport in a porous media

The mass transfer of fluid takes place through an interconnected network of pores. Porosity is defined as the volume of pore space per unit volume rock (Dullien, 2012). All rocks do have a small but finite porosity due to the crystal structure of adjoining grains that cannot fit perfectly together usually referred to as the degree of mismatch. This degree along with grain boundaries depend on the disparity between the structure and the orientation of the juxtaposed grains (Philpotts and Ague, 2009). For instance, if the lattice planes in adjoining crystals match then the grain boundaries are said to be coherent; if some lattice planes match then the grain boundaries are said to be semi-coherent; and if none match then it is incoherent (Osman, 2013). Hence, the more incoherent the boundary conditions are, the more space there is for the fluids to flow.

Fluid Motion

Groundwater has flow paths in which it moves in; the shortest path it can flow in can take a matter of days while the longest can take up to years (Anderson, 2007).

Groundwater can be stored in aquifers for thousands of years and even more without any outcropping issues (Schwartz and Ibaraki, 2011). An outcrop issue is a result of aquifer outcropping causing the stored fluid within to leak towards the surface (Ahmed, 2010).

The viscosity of water varies with dissolved solids within; however this variation was small compared to the other factors affecting the flow (Kirkham, 2005). In the upper crust, rocks have the significant strength to support the pore and fracture networks connected over several kilometres.

The density of the medium and liquid phase is a function of pressure, temperature, and contaminant concentration (Philpotts and Ague, 2009).

If the fluids were not able to escape the rock, the resulting increase in pressure would either force the grain boundaries open or cause hydro-fracturing or even result in both (Calabrese et al., 2005). The width of the channel increases as a result of the opening of grain boundaries. This increased width enables the easy of accommodating the growing flux of the fluid (Calabrese et al., 2005).

The volume flow rate per unit area of fluid passing through bulk rock can be calculated using Equation 5 (Whitaker, 1986).

$$J_Z = -\frac{K}{n}\left(\frac{\partial P}{\partial Z} + \rho g\right)$$

Equation 5: Darcy's law. Reproduced from (Whitaker, 1986).

where,

K is the permeability.

n is the viscosity.

J_Z is the volume of fluid passing.

Hydraulic fracturing

In the middle and lower crust, the large pressure difference at elevated temperature and pressure over long timescales result in fracturing the rock due to its inability to withstand such pressure as rocks can withstand no more than 0.03GPa of excess pressure (Philpotts and Ague, 2009). Due to their limited strength, rocks undergo recrystallization and ductile deformation which decreases the pore space around the fluids, restricts flow, and elevates fluid pressure to values close to the rock pressure. Under such conditions, the flow of fluid upwards towards the surface is strongly favoured (Ong, 2014). Hence, the max fluid pressure gradient can be estimated as the lithostatic gradient:

$$Fluid\ pressure\ gradient = -P_r * g$$

Equation 6: Fluid pressure gradient. Reproduced from (Philpotts and Ague, 2009).

where,

P_r is the density of the rock.

g is the acceleration due to gravity.

Due to its low viscosity, the fluid can flow through fractures or a series of interconnected pores. This was mentioned because any gain or loss of such a fluid can result in a change

in the bulk composition of the rock which might be a reason for the brine to outcrop (Myers, 2012).

Therefore, the lithostatic gradient needs to exceed the fluid pressure gradient to avoid hydraulic fracturing which will be checked in the modelling calculations to ensure that this assumption is met.

Explicit definition of Carter-Tracy function method

Carter and Tracy (1960) introduced a new technique that does not require the principle of superposition and allows direct calculations of water influx to reduce the complexity associated with Van Everdingen Hurst method as shown in Equation 7 (Qanbari and Clarkson, 2013).

The biggest limitation of the superposition concept is that it requires the skin factor which cannot be determined due to the wide range uncertainties accompanied with the variety of particles formed during the drilling operation (Stewart, 2011).

$$(W_e)_n = (W_e)_{n-1} + [(t_D)_n - (t_D)_{n-1}]\left[\frac{B\Delta p_n - (W_e)_{n-1}(P`_D)_n}{(P_D) - (t_D)_{n-1}(P`_D)_n}\right]$$

Equation 7: Carter and Tracy water influx equation. Reproduced from (Ahmed, 2010).

where,

B is the water influx constant.

t_D is the dimensionless time as shown in Equation 12.

n(n-1) is the current, previous, time step.

Δp_n is the total pressure drop.

P_D is the dimensionless pressure.

$P`_D$ is the dimensionless pressure derivative.

Strictly speaking, "Carter-Tracy functions" are a way of avoiding the need to include the whole of an enormous domain in a finite difference model (Fanchi, 2006). The idea was to include in the finite difference model just the crucial bit of the domain in the middle, and then use the Carter-Tracy method to predict the behaviour of the edge of that part of the domain, using analytical predictions of what happens in the surrounding region.

It is crucial to note that, Equation 7 describes the process in block of the aquifer; Equation 8 describes the flow mechanism, Equation 9 describes the pressure profile around the wellbore radius as a function of position and time, while Equations 10, 11, and 12 describe the boundary of the region studied in detail. The main difference between Carter-Tracy and Van Everdingen Hurst techniques is that the Carter-Tracy method assumes a constant water influx rate over each finite time interval (Dake, 2001).

$$B = 1.119 * \Phi * C_t * {r_e}^2 * h * f$$

Equation 8: Water influx constant. Reproduced from (Allard and Chen, 1988).

where,

Φ is the porosity.

C_t is the total reservoir compressibility, Psi^{-1}.

r_e is the radius of the aquifer.

h is the thickness of the aquifer.

f is the encroachment angle.

$$P(r_w, t) = P_i + \left[\frac{70.6 * -Q_b * \mu_b * B_w}{k * h}\right] * E_i \left[\frac{-948 * \Phi * \mu_b * C_t * {r_w}^2}{k * t}\right]$$

Equation 9: Ei-Function equation. Reproduced from (Eppelbaum and Kutasov, 2015).

where,

$P(r, t)$ is the pressure at a wellbore radius after a "t" amount of hours.

E_i is the exponential integral of radius also known as the line source solution.

r_w is the wellbore radius.

P_i is the initial pressure, Psi^{-1}.

h is the thickness of the aquifer, feet (ft).

Q_b is the flow rate, bbl/day.

$$P_D = \frac{370.529\sqrt{t_D} + 137.582t_D + 5.69549{t_D}^{1.5}}{328.834 + 265.488\sqrt{t_D} + 42.2157t_D + {t_D}^{1.5}}$$

Equation 10: Dimensionless pressure as a function of dimensionless time. Reproduced from (Edwardson et al., 1962).

where,

t_D is the dimensionless time.

$$P`_D = \frac{716.441 + 46.7984\sqrt{t_D} + 270.038t_D + 71.0098{t_D}^{1.5}}{1296.86\sqrt{t_D} + 1204.73t_D + 618.618{t_D}^{1.5} + 538.072{t_D}^2 + 142.41{t_D}^{2.5}}$$

Equation 11: Derivative of dimensionless pressure with respect to time. Reproduced from (Edwardson et al., 1962).

where,

t_D is the dimensionless time.

$$t_D = \frac{0.006328 * k * t}{\mu_b * \Phi * C_t * {r_e}^2}$$

Equation 12: Represents quantity referred to as the Dimensionless time. Reproduced from (McKinney, 2011).

where,

t is the time in days.

k is the permeability of aquifer, millidarcy (md).

C_t is the total reservoir compressibility, Psi^{-1}.

Φ is the porosity of the aquifer, (%).

μ_b is the viscosity of brine, centipoise (cp).

r_e is the radius of the aquifer, feet (ft).

Carter-Tracy Water Influx Model (Ahmed, 2010):

- Is not an exact solution to the diffusivity equation and should be considered as an approximation but by limiting the time-steps used in water influx calculations, it becomes a much better approximation to the Van Everdingen Hurst technique.

Carter-Tracy Water Influx Model	Van Everdingen-Hurst Model
Assumes constant water influx rates.	Does not assume constant water influx rates.
Does not require the superposition concept.	Involve tedious calculations as a result of superposition concept.

- Does not require the superposition concept.

Table 4: Comparison of the Carter-Tracy model with Van Everdingen-Hurst Model (Fanchi, 2006).

The proposed technique has the following advantages (Alghanim et al., 2012):

- Is entirely data driven and does not assume a priori functional form as other models resulting in a much more flexible model for self-adjustment to numerous range of data.
- Based on the dimensionless radius, time, and thickness.
- Simple, relatively easy to apply, and most importantly provides an accurate range of results.
- Consumes less computational time when compared to both traditional table lookup and other water influx calculation techniques such as Van Everdingen-Hurst Unsteady-State Model.
- Is considered as the best available technique for this particular case.

Description of the behaviour of liquid injected into a confined aquifer

A deep well aquifer model solves three joined partial differential equations that describe the behaviour of liquid injected into an aquifer (Nordbotten and Celia, 2006). The three differential equations are:

1. Conservation of total liquid mass;
2. Conservation of energy and momentum (Darcy);
3. Conservation of the mass of a particular contaminant dissolved in the waste injection fluid.

These equations describe the three-dimensional Darcy flow of a single-phase liquid in a porous aquifer. The second equation, conservation of energy, represents the convection and dispersion of energy in the confined aquifer which results from the injection of a fluid with different pressure and temperature to resident aquifer fluid (Menard and Grove, 1979). The last equation represents the hydrodynamic dispersion and convection within an aquifer. The physical principles which are considered as the assumptions of the model are found in Appendix C.

Assumptions accompanied with the equation used which limit the domain of applicability of method

Equation 7 is based on the following assumptions (Fanchi, 2000):

- Assumes constant water influx rates across each finite time interval.

Equation 8 is based on the following assumptions (Donnez, 2012):

- Uniform thickness and porosity.
- Constant permeability and total compressibility.
- The fluid is assumed to be encroaching in a radial form, $f = 360°$.

Equation 9 is based on the following assumptions (Donaldson et al., 1985):

- The well is injecting at a stable flow rate.
- The well is centred in a cylindrical reservoir of radius r_e.
- The reservoir is producing at uniform pressure P_i when production begins.
- No flow across the outer boundary, r_e.
- Exponential integral approximations include a cumulative error of about 0.75%.

Equations 10, 11, and 12 are based on the following assumptions (Slider, 1983):

- Constant permeability, total compressibility, porosity, and viscosity.

Results

Justification to why those specific initial values were chosen

Two initial pressure readings in the undisturbed aquifer before any injection takes place were studied:

- 100kPa
- 100MPa

The reason for selecting a lower limit pressure close to that of atmospheric pressure was because it is quite possible that thermo-chemical processes down there could have resulted in a partial vacuum. As for the purpose for the upper limit pressure being in the region of the relevant lithostatic pressure, so it was just short of causing natural fracking before anything is injected which would result in an approximated value of around 100MPa. See (Equation 6).

Three flow rate values were studied:

- 2 Mt/year
- 4 Mt/year
- 18Mt/year

The main purpose of studying three different flow rates was due to the various conditions of the aqueous solution. For instance according to Rojas and Asociados (2009), the PRC mine is expected to produce potassium chloride at a rate of around 2Mt/year but according to Titkov (2004) if the withdrawn aqueous solution was moderately cold, then there will be about twice as much sodium chloride as potassium chloride which would be around 4 Mt/year. However, Titkov (2004) also stated that if the aqueous solution's salt by mass concentration was about 20-25%, then the maximum required mass flow rate of brine associated with the disposal of all the waste in a single injection well would be around 18 Mt/year.

The viscosity and compressibility values were taken from the Handbook of Chemistry and Physics by Haynes (2015). The underground temperature at 3000 metres was assumed to be 353K. For the two initial pressure values, the compressibility of water and brine was assumed to be constant as there wasn't any significant change in the values as initial

pressure changed from 100kPa to 100MPa as shown in Table 5. However, that was not the case for the viscosity as it differed when the initial pressure changed as shown in Table 5. The rock compressibility was calculated using Equation 13 which related the pore compressibility with porosity to yield the following relation:

$$C_f = \left[\frac{1.782}{\Phi^{0.438}}\right] * 10^{-6}$$

Equation 13: Rock formation compressibility. Reproduced from (Hall, 1953).

where,

C_f is the formation compressibility, Psi-1.

Φ is the porosity, %.

Viscosity and Compressibility for 100kPa	Compressibility of brine Psi-1	Compressibility of water Psi-1	Viscosity of brine (cp)	Viscosity of water (cp)	Rock formation compressibility Psi-1
	5.81601E-14	7.25189E-14	6.97E-01	3.54E-01	3.60626E-06
Viscosity and Compressibility for 100MPa	Compressibility of brine Psi-1	Compressibility of water Psi-1	Viscosity of brine (cp)	Viscosity of water (cp)	Rock formation compressibility Psi-1
	5.81601E-14	7.25189E-14	0.759634768	0.385925	3.60626E-06

Table 5: Viscosity and Compressibility for 100kPa and 100MPa. Reproduced from (Haynes, 2005).

The geometry of the aquifer was measured using the stratigraphic diagram provided by Legarreta (1985) as shown in Appendix D. The thickness was calculated as the vertical distance from the top to the bottom of the aquifer; whereas the radius was computed as the horizontal distance from the location of injection to where the aquifer reached the surface as shown in Table 6. Furthermore, Ellard (2014) stated that the wellbore radius was 0.15 metres.

Radius		m	ft
	Wellbore	0.15	0.492126
	Aquifer	30000	98425.2
Thickness		m	ft
	Aquifer	11.78571429	38.66704286

Table 6: Geometry of the confined cylindrical aquifer.

The permeability and porosity values used in the calculations are shown in Table 7.

	Permeability m^2 (Higher limit)	Permeability m^2 (Lower limit)	Porosity %
Sandstone	1E-13	1E-17	0.2
Limestone and Dolomite	1E-13	1E-16	0.15
Silty sand	1E-10	1E-14	0.5

Table 7: Permeability and Porosity values used in the calculations. Reproduced from (Nonner, 2015; Qiao and li, 2014)

A 3D-model was constructed using Groundwater Modelling System for illustrating the geometry of the confined aquifer potential for the disposal of waste brine as shown in Figure 3 (Rink et al., 2011).

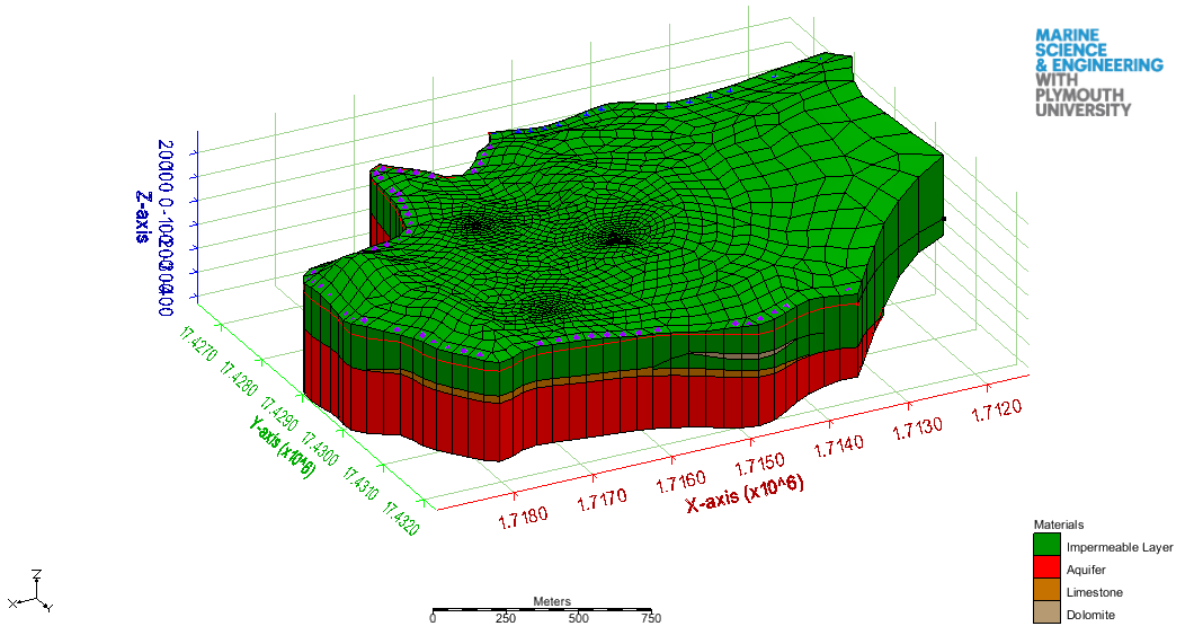

Figure 3: 3D-model of the confined aquifer potential for the disposal of waste brine for illustration purposes.

Step by step guide to understanding the calculations:

Before diving into the calculation's guide, it is important to comprehend the way the calculations were constructed. Figure 4 explains the way the calculations were constructed.

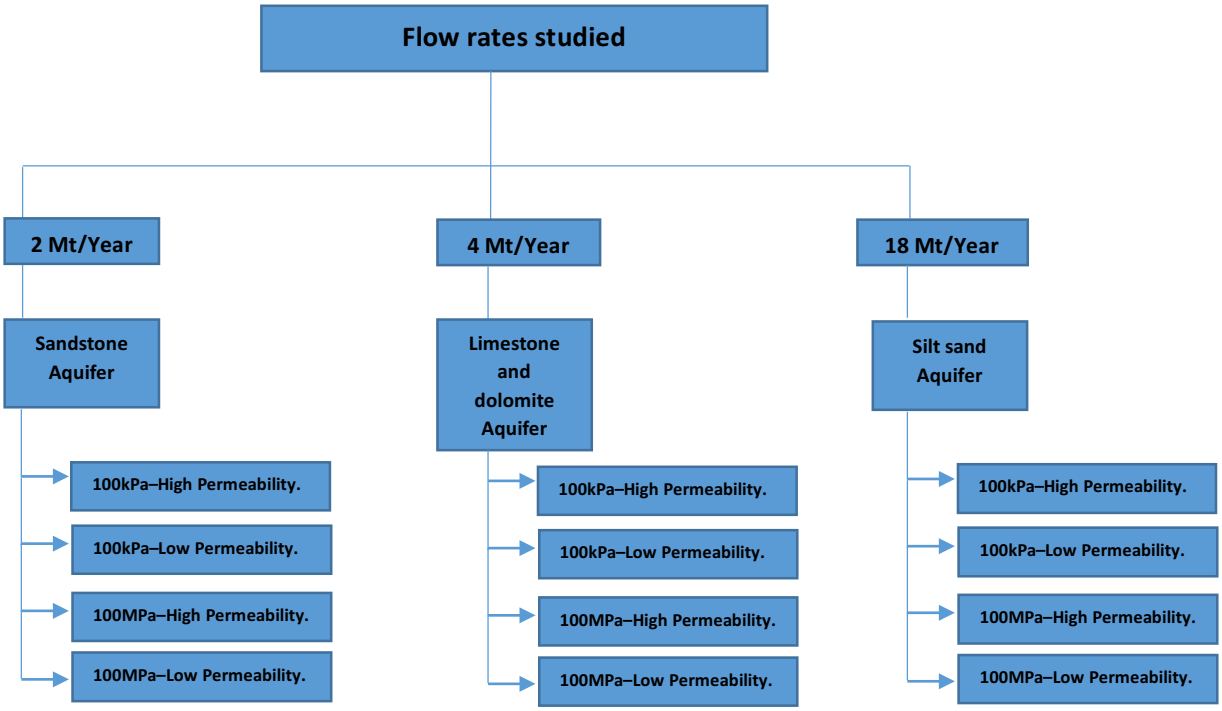

Figure 4: Clarifying how the calculations were constructed.

The purpose of conducting this study to include the different permeability values shown in Table 7 was to examine the effect of low and high permeability on both the cumulative water influx and calculated flows rates using Equations 7 and 14 respectively. Furthermore,

this is because the detailed measurements of the actual permeability of this aquifer are unavailable.

The units were converted from SI to oilfield units using Table 16 as shown in Appendix A. The lack of standardised units in such a matter is very risky as converting the units might result in a slight variation in the calculations yielding to a propagated error that was not accounted for (Ti et al., 1995).

Step 1:

It should be noted that the demonstrated results reflect the 2Mt/year flow rate (100kPa-Low Permeability aquifer). The pressure profile at the specified wellbore radius (0.492126 feet) was calculated using Equation 9 combined with the finite difference method set out in Equation 7 for a long duration of time that started from 1 hour up to 10 years as shown in Table 8. The main reason for having a long duration with limited time-steps was to improve the accuracy of the Carter-Tracy method. The pressure at wellbore as a function of time was plotted on a semi-log scale, as shown in Figure 5. Once the pressure at the wellbore radius was calculated for the specified timescale, the pressure drop was calculated as shown in Table 8 and then plotted as shown in Figure 6.

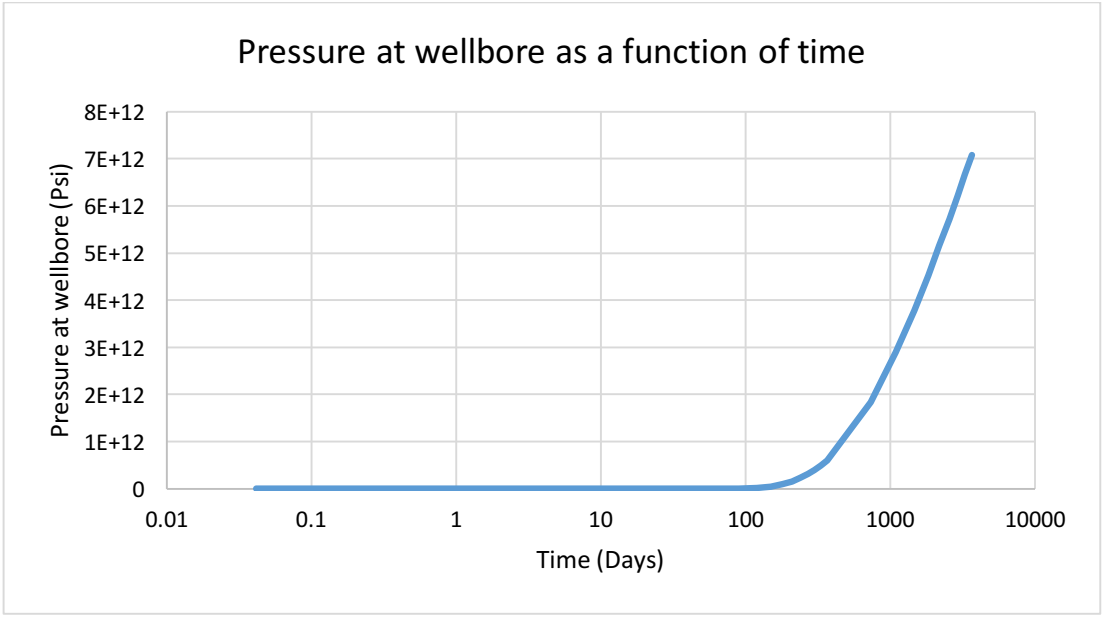

***Figure 5**: Pressure at wellbore as a function of time.*

Radius (feet)	Time (Days)	Pressure (Psi)	Pressure drop ΔP
0.492126	0	14.50377378	0
0.492126	0.041666667	14.50377378	0
0.492126	0.083333333	14.50377378	0
0.492126	0.125	14.50377378	0
0.492126	0.166666667	14.50377378	0
0.492126	0.208333333	14.50377378	0
0.492126	0.25	14.50377378	0
0.492126	0.291666667	14.50377378	0
0.492126	0.333333333	14.50377378	0
0.492126	0.375	14.50377378	0
0.492126	0.416666667	14.50377378	0
0.492126	0.458333333	14.50377378	0
0.492126	0.5	14.50377378	0
0.492126	1	14.50377378	0
0.492126	2	14.50377378	0
0.492126	3	14.50377378	0
0.492126	15	14.50377378	0
0.492126	30	14.50377378	0
0.492126	60	185899023.4	-92949504.42
0.492126	90	3723246132	-1861623059
0.492126	120	17813523347	-8813812162
0.492126	150	47316034211	-21796394039
0.492126	180	91431892737	-36809184695
0.492126	210	1.52186E+11	-52434826935
0.492126	240	2.2525E+11	-66909129989
0.492126	270	3.07063E+11	-77438450428
0.492126	300	3.95627E+11	-85188356528
0.492126	330	4.89368E+11	-91152758369
0.492126	365	6.03509E+11	-1.03941E+11
0.492126	730	1.83511E+12	-6.72872E+11
0.492126	1095	2.89799E+12	-1.14724E+12
0.492126	1460	3.77872E+12	-9.71802E+11
0.492126	1825	4.52205E+12	-8.12029E+11
0.492126	2190	5.16271E+12	-6.91997E+11
0.492126	2555	5.72477E+12	-6.01362E+11
0.492126	2920	6.22503E+12	-5.3116E+11
0.492126	3285	6.67555E+12	-4.75389E+11
0.492126	3650	7.08522E+12	-4.30092E+11

Table 8: Calculated pressure values at wellbore radius.

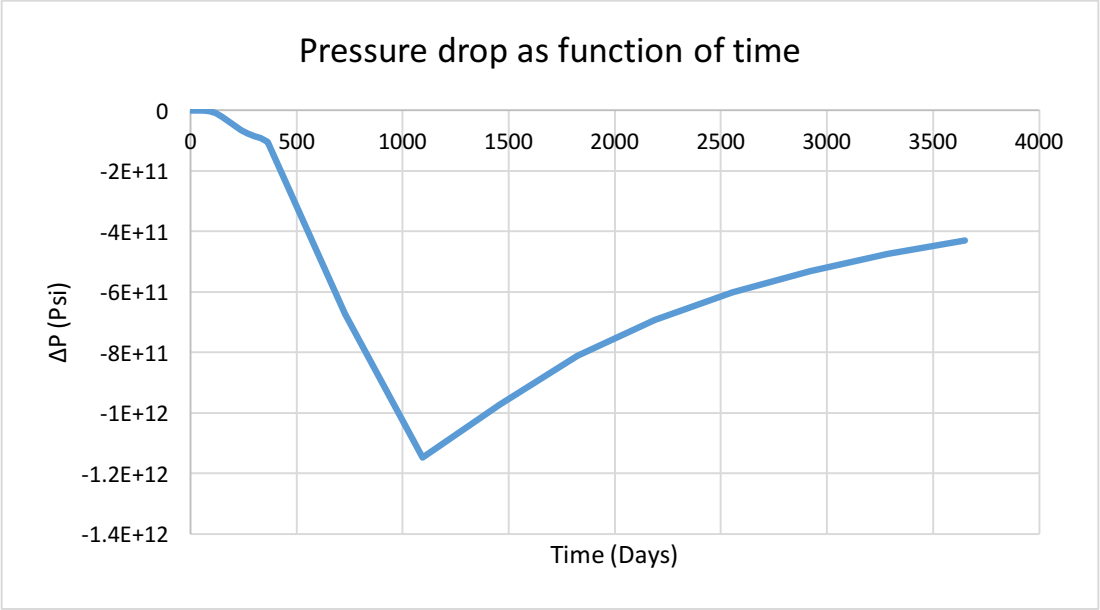

Figure 6: Pressure difference between the edge of the aquifer and wellbore as a function of time.

Step 2

The water influx constant was calculated using Equation 8. The calculated water influx constant was: $B = 302322.3336\ bbl/Psi$.

Step 3

Once the water influx constant was calculated, the dimensionless time was calculated using Equation 12. After the dimensionless time had been calculated, the dimensionless pressure and derivative of dimensionless pressure were then computed using Equations 10 and 11 respectively. The results of the calculated dimensionless values are shown in Table 9. The dimensionless pressure against dimensionless time was plotted as shown in Figure 7.

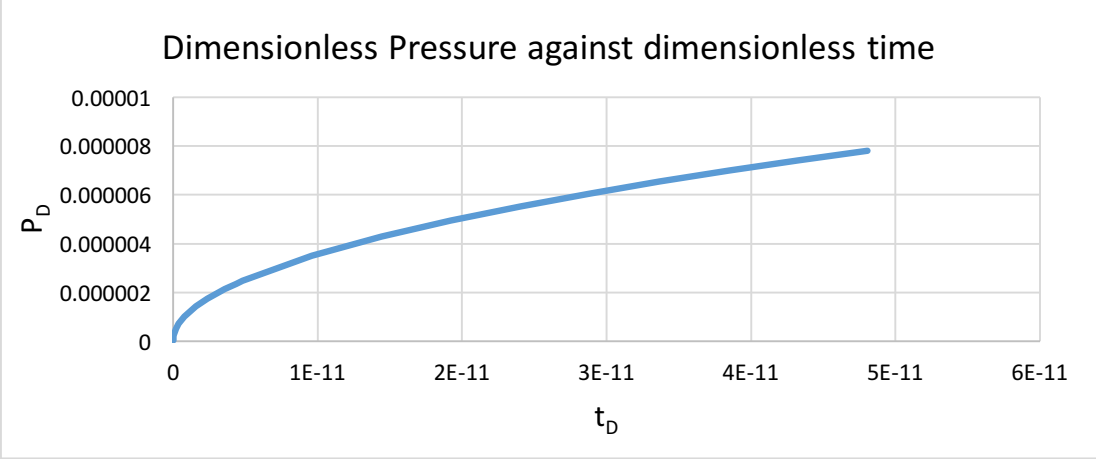

Figure 7: Dimensionless Pressure against dimensionless time.

Dimensionless Time t_D	Dimensionless Pressure P_D	Derivative of Dimensionless Pressure P_D'
0	0	0
5.48664E-16	2.63936E-08	23584803.22
1.09733E-15	3.73262E-08	16676974.15
1.64599E-15	4.5715E-08	13616692.29
2.19465E-15	5.27872E-08	11792401.37
2.74332E-15	5.90179E-08	10547444.38
3.29198E-15	6.46508E-08	9628455.313
3.84064E-15	6.98309E-08	8914217.423
4.38931E-15	7.46524E-08	8338486.836
4.93797E-15	7.91808E-08	7861600.755
5.48664E-15	8.34639E-08	7458169.308
6.0353E-15	8.75376E-08	7111085.397
6.58396E-15	9.14301E-08	6808345.904
1.31679E-14	1.29302E-07	4814227.418
2.63359E-14	1.8286E-07	3404172.714
3.95038E-14	2.23957E-07	2779495.294
1.97519E-13	5.00783E-07	1243027.82
3.95038E-13	7.08214E-07	878953.2612
7.90076E-13	1.00157E-06	621513.6716
1.18511E-12	1.22666E-06	507463.7003
1.58015E-12	1.41643E-06	439476.3921
1.97519E-12	1.58361E-06	393079.5845
2.37023E-12	1.73476E-06	358830.884
2.76526E-12	1.87376E-06	332212.8094
3.1603E-12	2.00313E-06	310756.5973
3.55534E-12	2.12464E-06	292984.1023
3.95038E-12	2.23957E-06	277949.1
4.34542E-12	2.34888E-06	265014.0464
4.80629E-12	2.4703E-06	251987.7278
9.61259E-12	3.49353E-06	178182.0914
1.44189E-11	4.27869E-06	145484.9808
1.92252E-11	4.9406E-06	125993.6253
2.40315E-11	5.52376E-06	112692.074
2.88378E-11	6.05097E-06	102873.2768
3.3644E-11	6.5358E-06	95242.11197
3.84503E-11	6.98706E-06	89090.80713
4.32566E-11	7.41089E-06	83995.5912
4.80629E-11	7.81177E-06	79685.19

Table 9: Calculated dimensionless values.

Step 4

Once the water influx constant and all the dimensionless values were calculated, the cumulative water influx values were then calculated using Equation 7 as shown in Table 10. The cumulative water influx helped give an idea of the amount of water that will be stored in the confined aquifer using the given production rates. A plot of cumulative water influx against time was achieved as shown in Figure 8.

W_e (bbl) (radius: 98425.2 ft)
0
0
0
0
0
0
0
0
0
0
0
0
0
0
0
0
0
-14682784.51
-280372963.9
-1401351391
-3879832415
-7628454129
-12471413739
-18119108748
-24084851013
-30101808445
-36042698296
-43529475466
-4.00142E+11
-8.81775E+11
-1.16287E+12
-1.32671E+12
-1.42438E+12
-1.48291E+12
-1.51721E+12
-1.53592E+12
-1.54433E+12

Table 10: Calculated cumulative water influx values.

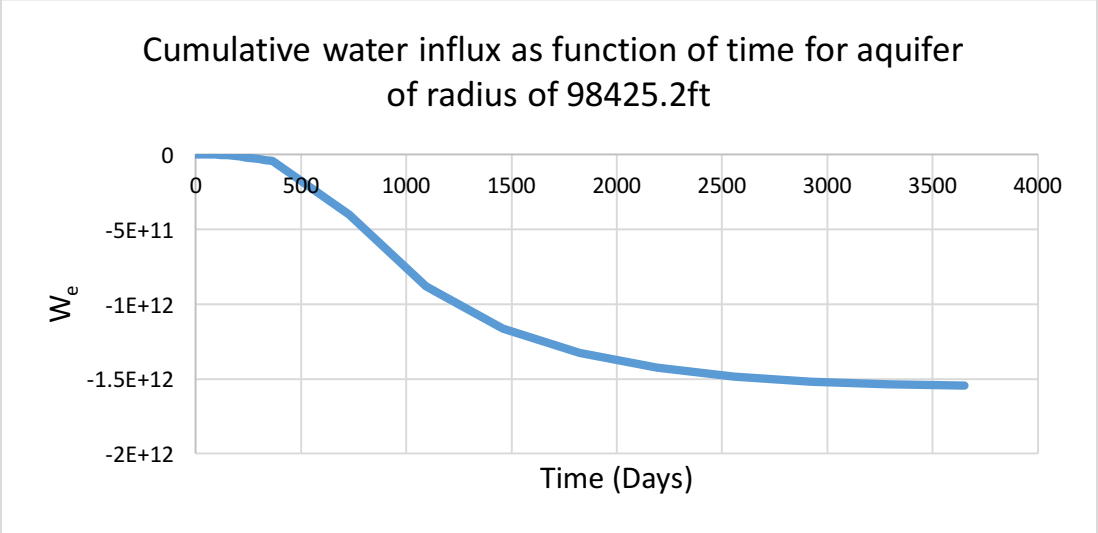

Figure 8: Cumulative water influx against time.

The reason the cumulative water influx values are negative was simply because the aqueous solution is being injected into the aquifer not extracted out.

Step 5

Determining whether the brine leaks out at outcrop was done by using Darcy's radial flow for incompressible fluids as shown in Equation 14:

$$q = \frac{-0.00708 * k * h * (P_e - P_w)}{\mu * B * \ln\left[\frac{r_e}{r_w}\right]}$$

Equation 14: Darcy's radial flow for incompressible fluids. Reproduced from (Ezekwe, 2011).

where,

P_e is the initial pressure.

P_w is the maximum calculated pressure.

r_e is the radius of the aquifer.

r_w is the wellbore radius.

The results of Equation 14, shown in Table 11, reflect the all various conditions for the 2Mt/year flow rate, not just the 100kPa-Low Permeability aquifer as stated in Step 1. The calculated flow rates for the different conditions studied are plotted as shown in Figure 9.

The same process was repeated for both the 4Mt/year and 18Mt/year flow rates and plotted as shown in Figures 10 and 11 respectively.

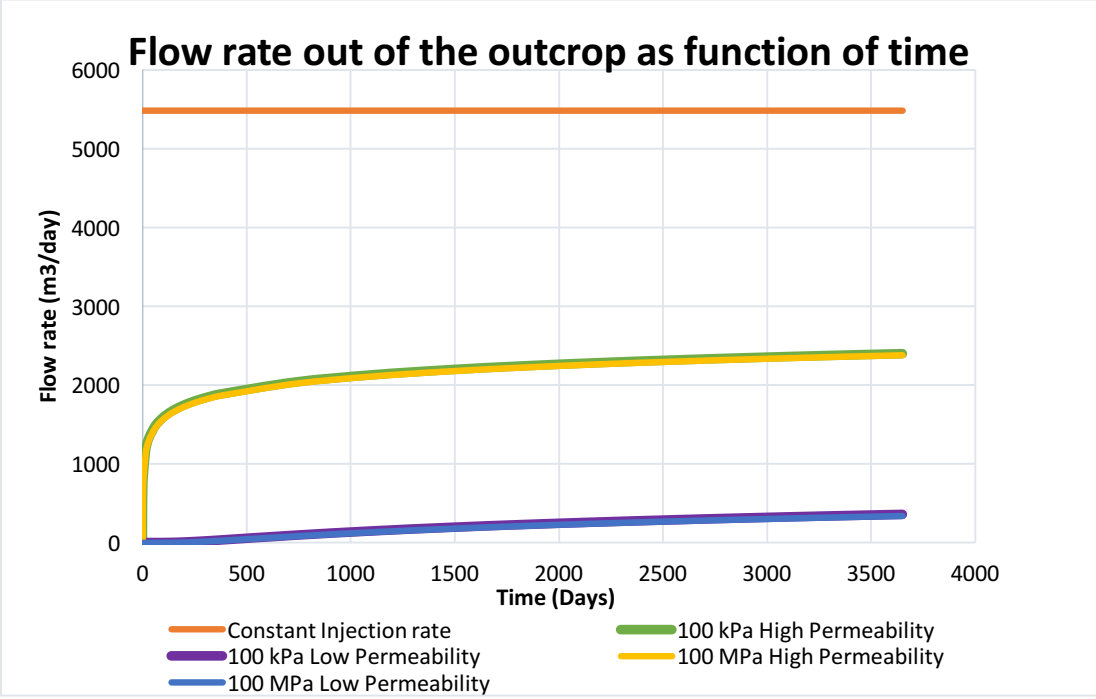

Figure 9: Calculated flow rates (2 Mt/year) for various conditions studied as a function of time.

Time (Days)	Constant Injection rate (m^3/day)	100kPa - High Permeability - Flow rate (m^3/day)	100kPa - Low Permeability - Flow rate (m^3/day)	100MPa - High Permeability - Flow rate (m^3/day)	100MPa - Low Permeability - Flow rate (m^3/day)
-	-	-	-	-	-
0.041666667	5479.45223	39.14032582	0	33.24887952	0
0.083333333	5479.45223	108.5138888	0	97.8111519	0
0.125	5479.45223	165.600445	0	152.5732949	0
0.166666667	5479.45223	212.008436	0	197.6355253	0
0.208333333	5479.45223	250.7761615	0	235.5256994	0
0.25	5479.45223	283.9743709	0	268.1059902	0
0.291666667	5479.45223	312.9697766	0	296.6426132	0
0.333333333	5479.45223	338.6925503	0	322.0113418	0
0.375	5479.45223	361.7991719	0	344.8366037	0
0.416666667	5479.45223	382.7684655	0	365.5770837	0
0.458333333	5479.45223	401.9597147	0	384.5787595	0
0.5	5479.45223	419.6491008	0	402.108658	0
1	5479.45223	564.9947172	0	546.5644438	0
2	5479.45223	715.236016	0	696.3718835	0
3	5479.45223	800.9691139	0	781.6114963	0
15	5479.45223	1162.107274	0	1142.749656	0
30	5479.45223	1317.641014	0	1298.283396	0
60	5479.45223	1473.174753	0.009352763	1453.817136	0.00424159
90	5479.45223	1564.156159	0.187320194	1544.798541	0.108044317
120	5479.45223	1628.708493	0.896215976	1609.350875	0.583429717
150	5479.45223	1678.779173	2.380516476	1659.421556	1.66741502
180	5479.45223	1719.689898	4.600028948	1700.332281	3.453770396
210	5479.45223	1754.279423	7.656612477	1734.921806	5.793912582
240	5479.45223	1784.242233	11.33255795	1764.884615	8.846298554
270	5479.45223	1810.671304	15.44862253	1791.313686	12.35158052
300	5479.45223	1834.312913	19.90437889	1814.955296	16.20218992
330	5479.45223	1855.69935	24.62059338	1836.341733	20.32603545
365	5479.45223	1878.318691	30.36314135	1858.961073	25.40333774
730	5479.45223	2033.85243	92.32631111	2014.494813	82.49826783
1095	5479.45223	2124.833836	145.8006408	2105.476218	133.492078
1460	5479.45223	2189.38617	190.1109636	2170.028552	176.3406533
1825	5479.45223	2239.456851	227.5086425	2220.099233	212.7762886
2190	5479.45223	2280.367575	259.741119	2261.009958	244.3272128
2555	5479.45223	2314.9571	288.0189177	2295.599483	272.0966485
2920	5479.45223	2344.91991	313.1875346	2325.562292	296.8714682
3285	5479.45223	2371.348981	335.8535053	2351.991363	319.2234526
3650	5479.45223	2394.99059	356.4642496	2375.632973	339.5780876

Table 11: Calculated flow rates at the edge of the aquifer where outcropping may take place at specified times.

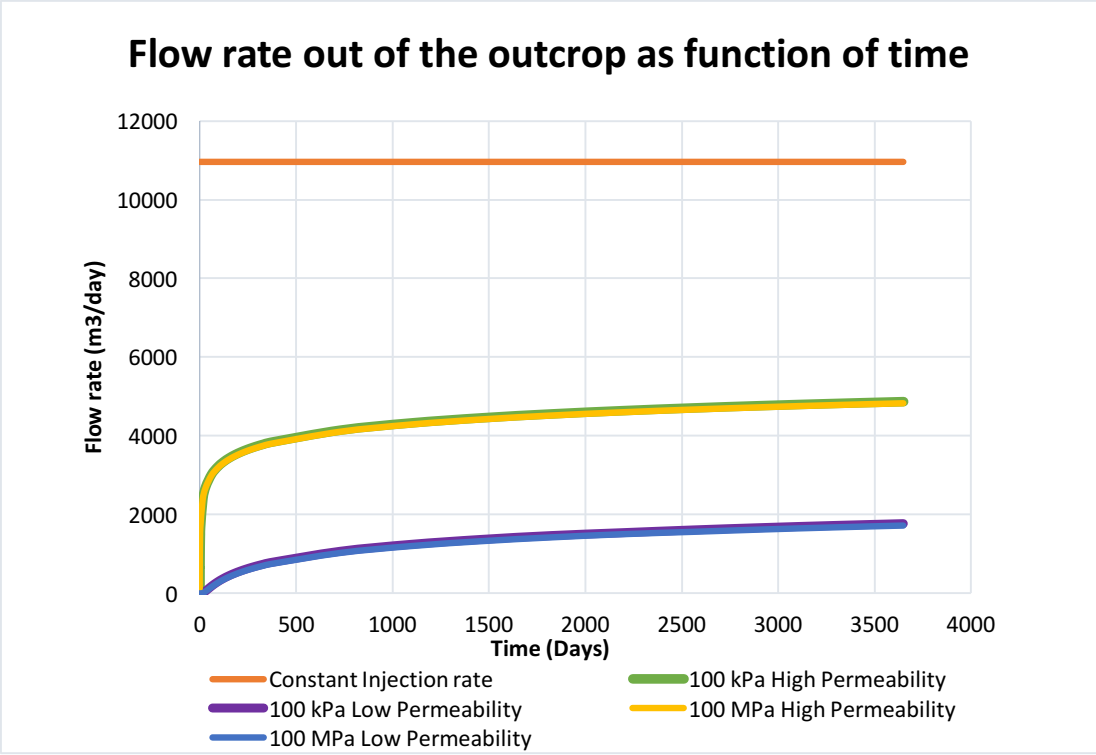

Figure 10: Calculated flow rates (4 Mt/year) for various conditions studied as a function of time.

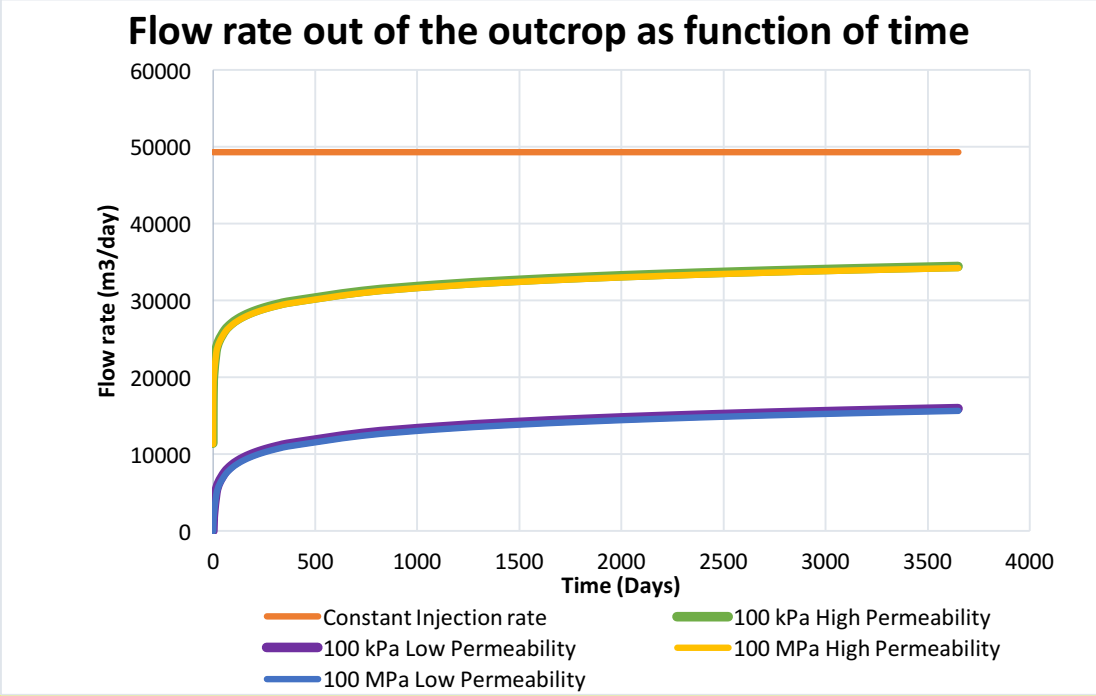

Figure 11: Calculated flow rates (18 Mt/year) for various conditions studied as a function of time.

The effect of varying permeability values could be noticed as when the low permeability value was chosen, the flow rates for both 100kPa and 100MPa were zero up to the 30th day but that was not the case when the high permeability value was chosen. Furthermore by looking at Figures 9, 10, and 11, it was noticed that the flow rate out of the outcrop was affected when the initial pressure changed but on a small scale, however, when the permeability values changed, the flow rate out of the outcrop changed massively.

By looking at the results shown in Table 11, it was noticed that all the results were highly positive which gave an indication that there was a significant outward radial component of Darcy's velocity which meant that not only brine will be leaking from the aquifer but also brine will be leaking at high rates and this is all due to the high production rates set by Vale. Therefore, the brine stored within the aquifer will eventually outcrop to the surface.

The maximum pressure required to cause hydraulic fracturing was calculated using Equation 6. The result of this calculation was $2000(density) * 10(gravity) * 3000(depth) = 60MPa$. The depth was assumed based on that fact the surface is deeper than the evaporative layer; the density was assumed based on the typical density of rock. The reason for the assumptions was because the detailed information was unavailable. When comparing 60MPa with the high values presented in Table 8, it was clear that fracking will be occurring due to the high injection rates.

Therefore, the issue is now even bigger as brine not only outcrops from the aquifer but also the impermeable layer will fracture leading to contaminating the groundwater in nearby aquifers.

The drawn conclusion of the aquifer outcropping was based on the stratigraphic diagram of the permeable and impermeable layer provided by Legarreta (1985) as shown in Appendix D. However, the author of the stratigraphic diagram has not made it clear that the upper boundary of the diagram is the ground-surface leaving some doubt.

Therefore, if the layer treated as the surface was another impermeable layer instead of being the surface there might still be a chance for the aquifer to outcrop but if an impermeable layer with negligible thickness was present, then even if the brine leaked out of the aquifer it will eventually get trapped within the impermeable layer.

Validation

The application of Van Everdingen-Hurst method that has been compared in this section was based on a set of results that has already been published in a peer-reviewed journal, and the present author has applied the Carter-Tracy method, by limiting the time-steps to less than 30 days, for the same situation for comparison purposes.

Using the peer-reviewed information in Tables 12 and 13, the cumulative water influx was calculated using the Carter-Tracy method and then compared to Van Everdingen-Hurst method as shown in Table 14.

Property	Porosity (ϕ)	Total compressibility (C_t)	Permeability (K)	Thickness (h)	Viscosity (μ)	Radius of reservoir (r_e)	Encroachment Angle (f)
Unit	%	Psi^{-1}	md	ft	cp	ft	Degrees (°)
Value	23	0.000007	2180	212	0.1728	6561.6797	0.444444444

Table 12: Estimated properties of the aquifer. Reproduced from (John and Friday, 2011).

N	Time (days)	Pressure (Psia)
0	0	3452.3
1	365	3328.8
2	728	3263.91
3	1090	3142.93
4	1455	2999.57
5	1820	2870.8
6	2185	2758.08
7	2551	2697.49

Table 13: Pressure history at the aquifer boundary. Reproduced from (John and Friday, 2011).

N	Time (days)	Pressure (Psia)	Calculated (W_e) Carter-Tracy method (bbl)	Calculated (W_e) Van Everdingen-Hurst (bbl)
0	0	3452.3	0	0
1	365	3328.8	55326687.79	63057231.92
2	728	3263.91	79619261.02	209342476.9
3	1090	3142.93	126834556.6	427474222.2
4	1455	2999.57	181803933.1	754586564.6
5	1820	2870.8	229156657.5	1185013265
6	2185	2758.08	269099916.2	1697860109
7	2551	2697.49	288037734.1	2250770727

Table 14: Compassion between results of the Carter-Tracy water influx calculations with those of the Van Everdingen-Hurst method.

The comparison shown in Table 14 indicates that the Carter-Tracy method significantly overestimates the water influx. This overestimation was due to the substantial time-step of 1 year used to calculate the water influx. As previously stated, the precision of the Carter-Tracy method was improved by limiting the time-step utilised in determining the water influx to less than 30 days. Therefore, the water influx was then recalculated on a monthly basis as shown in Table 15.

Time (days)	Pressure (Psia)	Pressure drop ΔP (Psi)	Dimensionless Time t_D	Dimensionless Pressure P_D	Derivative of dimensionless Pressure P_D'	Calculated (W_e) Carter-Tracy method (bbl)
0	3452.3	0	0	0	0	0
30	3448.922	3.378	34.54972147	2.213089435	0.013621694	385429.1793
60	3439.652	12.648	69.09944294	2.543644516	0.006983497	1732212.996
90	3430.382	21.918	103.6491644	2.725040889	0.004823966	3925574.765
120	3421.112	31.188	138.1988859	2.868881925	0.003617974	6886693.966
150	3411.842	40.458	172.7486073	2.9804537	0.002894379	10578876.28
180	3402.572	49.728	207.2983288	3.071614479	0.002411983	14976476.21
210	3393.302	58.998	241.8480503	3.148689819	0.002067414	20060085.62
240	3384.032	68.268	276.3977718	3.215455515	0.001808987	25814248.61
270	3374.762	77.538	310.9474932	3.274347033	0.001607989	32226213.37
300	3365.492	86.808	345.4972147	3.327027291	0.00144719	39285182.33
330	3356.222	96.078	380.0469362	3.374682381	0.001315627	46981829.4
360	3346.952	105.348	414.5966576	3.418188069	0.001205991	55307972.34
365	3345.407	106.893	420.3549445	3.42508473	0.001189471	56713128.56
395	3336.137	116.163	454.904666	3.464578936	0.001099131	65765095.43
425	3326.867	125.433	489.4543875	3.501180638	0.001021546	75431684.74
455	3317.597	134.703	524.004109	3.535284763	0.000954191	85707084.24
485	3308.327	143.973	558.5538304	3.567210499	0.000895169	96585983.13
515	3299.057	153.243	593.1035519	3.597219504	0.000843023	108063498.4
545	3289.787	162.513	627.6532734	3.625528951	0.000796618	120135115.9
575	3280.517	171.783	662.2029948	3.652321074	0.000755055	132796642.5
605	3271.247	181.053	696.7527163	3.677750282	0.000717615	146044166.9
635	3261.977	190.323	731.3024378	3.701948553	0.000683712	159874026.3
665	3252.707	199.593	765.8521592	3.725029574	0.000652868	174282779.9
695	3243.437	208.863	800.4018807	3.747091976	0.000624686	189267184.5
725	3234.167	218.133	834.9516022	3.768221881	0.000598837	204824175.4
728	3233.24	219.06	838.4065743	3.770286578	0.000596369	206385600.2
758	3223.97	228.33	872.9562958	3.790477746	0.000572766	222569241.4
788	3214.7	237.6	907.5060173	3.809885098	0.000550961	239319532
818	3205.43	246.87	942.0557387	3.828567222	0.000530754	256633861.2
848	3196.16	256.14	976.6054602	3.846576371	0.000511977	274509739
878	3186.89	265.41	1011.155182	3.86395935	0.000494484	292944786.3
908	3177.62	274.68	1045.704903	3.880758243	0.000478146	311936726.4
938	3168.35	283.95	1080.254625	3.897011028	0.000462854	331483376.9
968	3159.08	293.22	1114.804346	3.912752097	0.000448509	351582642.9
998	3149.81	302.49	1149.354068	3.928012692	0.000435027	372232511.1
1028	3140.54	311.76	1183.903789	3.942821276	0.000422332	393431043.4
1058	3131.27	321.03	1218.453511	3.95720386	0.000410356	415176372.7
1088	3122	330.3	1253.003232	3.971184267	0.000399041	437466697.8
1090	3121.382	330.918	1255.306547	3.972102541	0.000398309	438955141.9
1120	3112.112	340.188	1289.856268	3.985678036	0.00038764	461824945
1150	3102.842	349.458	1324.40599	3.998894664	0.000377528	485236211.2
1180	3093.572	358.728	1358.955711	4.011770912	0.00036793	509187317.5
1210	3084.302	367.998	1393.505433	4.024323873	0.000358807	533676692.3
1240	3075.032	377.268	1428.055154	4.036569383	0.000350127	558702812.3
1270	3065.762	386.538	1462.604876	4.048522143	0.000341856	584264199.8
1300	3056.492	395.808	1497.154597	4.060195825	0.000333967	610359420.4
1330	3047.222	405.078	1531.704318	4.071603164	0.000326434	636987080.7
1360	3037.952	414.348	1566.25404	4.082756043	0.000319233	664145826.2
1390	3028.682	423.618	1600.803761	4.093665566	0.000312343	691834339
1420	3019.412	432.888	1635.353483	4.104342129	0.000305744	720051336.8
1450	3010.142	442.158	1669.903204	4.114795471	0.000299419	748795570.4
1455	3008.597	443.703	1675.661491	4.116516643	0.00029839	753600918.9
1485	2999.327	452.973	1710.211213	4.126721079	0.000292362	782958826
1515	2990.057	462.243	1744.760934	4.136721412	0.000286572	812841367.2
1545	2980.787	471.513	1779.310656	4.146525648	0.000281008	843247389.6
1575	2971.517	480.783	1813.860377	4.156141329	0.000275655	874175767.7
1605	2962.247	490.053	1848.410099	4.165575571	0.000270503	905625402.3
1635	2952.977	499.323	1882.95982	4.174835095	0.000265539	937595219.6
1665	2943.707	508.593	1917.509542	4.183926255	0.000260755	970084169.9
1695	2934.437	517.863	1952.059263	4.192855063	0.00025614	1003091227
1725	2925.167	527.133	1986.608985	4.201627218	0.000251685	1036615386
1755	2915.897	536.403	2021.158706	4.210248121	0.000247383	1070655665
1785	2906.627	545.673	2055.708427	4.218722901	0.000243225	1105211101
1815	2897.357	554.943	2090.258149	4.227056427	0.000239205	1140280752
1820	2895.812	556.488	2096.016436	4.228431943	0.000238548	1146139975
1850	2886.542	565.758	2130.566157	4.236606512	0.000234679	1181808455
1880	2877.272	575.028	2165.115879	4.244649581	0.000230935	1217989171
1910	2868.002	584.298	2199.6656	4.252565314	0.000227307	1254681239
1940	2858.732	593.568	2234.215322	4.260357679	0.000223792	1291883791
1970	2849.462	602.838	2268.765043	4.268030464	0.000220384	1329595977
2000	2840.192	612.108	2303.314765	4.275587283	0.000217078	1367816960
2030	2830.922	621.378	2337.864486	4.283031589	0.00021387	1406545922
2060	2821.652	630.648	2372.414208	4.290366684	0.000210756	1445782058
2090	2812.382	639.918	2406.963929	4.297595726	0.000207731	1485524576
2120	2803.112	649.188	2441.513651	4.304721737	0.000204791	1525772700
2150	2793.842	658.458	2476.063372	4.311747614	0.000201933	1566525666
2180	2784.572	667.728	2510.613093	4.318676131	0.000199155	1607782723
2185	2783.027	669.273	2516.37138	4.319821607	0.000198699	1614672901
2215	2773.757	678.543	2550.921102	4.326639895	0.000196008	1656517195
2245	2764.487	687.813	2585.470823	4.333366454	0.000193388	1698863996
2275	2755.217	697.083	2620.020545	4.340003719	0.000190838	1741712592
2305	2745.947	706.353	2654.570266	4.346554031	0.000188354	1785062283
2335	2736.677	715.623	2689.119988	4.353019638	0.000185934	1828912378
2365	2727.407	724.893	2723.669709	4.359402704	0.000183576	1873262200
2395	2718.137	734.163	2758.219431	4.365705308	0.000181276	1918111079
2425	2708.867	743.433	2792.769152	4.371929455	0.000179034	1963458359
2455	2699.597	752.703	2827.318874	4.378077074	0.000176846	2009303390
2551	2697.49	754.81	2937.877982	4.397256413	0.000170191	2155396383

Table 15: Recalculated water influx values on a monthly basis using the Carter-Tracy method.

The recalculated water influx values shown in Table 15 should be considered as the best match when being compared to the Van Everdingen Hurst method as illustrated in Figure 12.

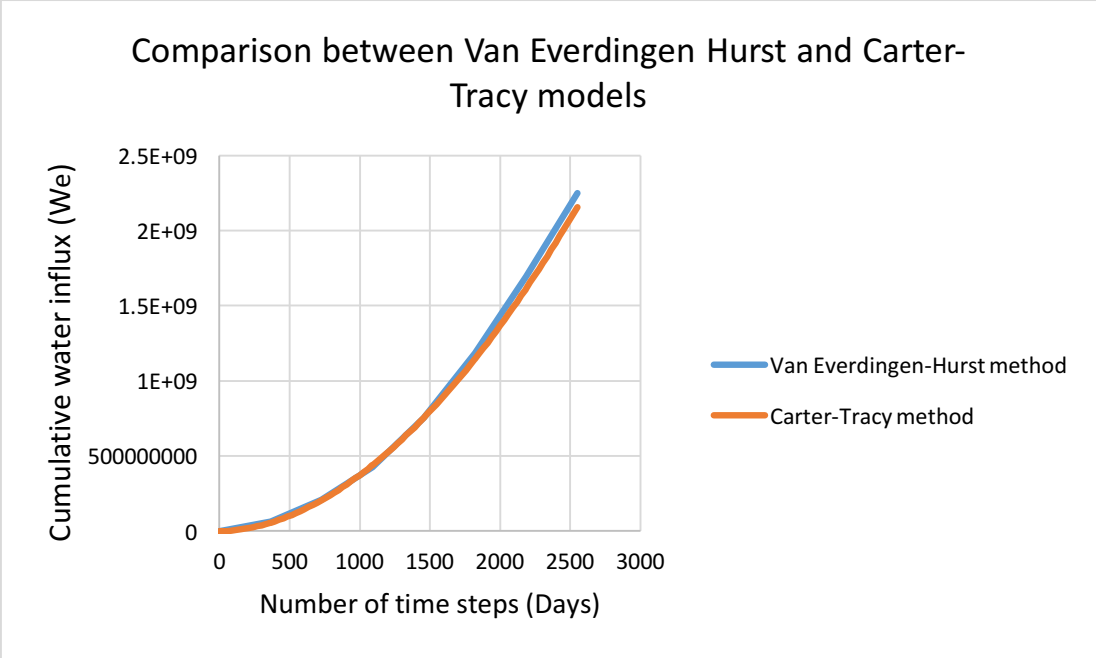

Figure 12: Comparison between Van Everdingen Hurst and Carter-Tracy models.

Looking at Figure 12, it could be noticed that there is a slight disparity between the two methods. The reason for this was due to the difference in the equations used to describe the dimensionless time which yielded a propagated variation of around 0.032% as shown in Equations 15 and 16. This small difference could not be noticed at the start as the effects of this variation started appearing at the higher time-steps (2000 → 2500) as shown in Figure 12.

$$t_D = \frac{0.006328 * k * t}{\mu_b * \Phi * C_t * {r_e}^2}$$

Equation 15: Dimensionless time using Carter-Tracy method. Reproduced from (McKinney, 2011).

$$t_D = \frac{0.00633 * k * t}{\mu_b * \Phi * C_t * {r_e}^2}$$

Equation 16: Dimensionless time using Van Everdingen-Hurst method. Reproduced from (John and Friday, 2011).

Based on the critical evaluation of the validated results, a point has been proven here that the Carter-Tracy method can be used to determine the water influx and it is capable of producing reliable results by limiting the time-step to less than 30 days. Furthermore, the Van Everdingen-Hurst method should not be used for this specific case because some data that should not be assumed such as, segregation drive index, injection drive index, and skin factor; and if they were assumed, that would lead to an additional source of error.

Therefore, the Carter-Tracy method should be considered as the best available technique for this specific problem not only because it eliminates the need for the principle of superposition but also due to the limited timescale of the project.

Conclusion

Human activities such as waste disposal, agricultural practices, and solution mining have negatively affected the quality of groundwater. For instance, more than one-third of the world's irrigated land is affected by soil salinisation and this condition poses a threat to environmental conservation and food security. This project focused on the disposal of strong waste brine in a deep saline cylindrical confined aquifer to help solve a major societal problem, groundwater contamination. After conducting documentary research on groundwater hydrology, diffusive transport, physics of groundwater storage, fluid storage and transport in porous media, it was found that the Carter-Tracy method was the best available technique for this specific problem not only because of the wide range of uncertainties accompanied with the model but mainly due to the advantages described. The Carter-Tracy was used to determine the cumulative water influx rates at any given time, as shown in Table 10, which enabled carrying out the calculation to determine whether hydraulic fracturing would occur within the region of study (PRC mine).

The Carter-Tracy technique has verified that strong-waste brine could be stored in a deep saline cylindrical confined aquifer but the result of the hydraulic fracturing calculation was 60MPa and when comparing the 60 MPa with high values presented in Table 8, it was evident that hydraulic fracturing will be occurring.

Determining whether brine leaks out at outcrop was done by using Darcy's radial flow for incompressible fluids as shown in Equation 14. The positive results of Equation 14 shown in Table 11 were evident to verify that brine will be leaking out at very high rates with the lowest being 356.5 m^3/day and highest being 2395 m^3/day.

This meant that waste brine will not only be leaking out at high rates but also has additional paths to leak towards the surface, due to the fractured rocks, making it easier to contaminate groundwater stored in the surrounding aquifers. However, it must be noted that the drawn conclusion was based on the stratigraphic diagram of the permeable and impermeable layer provided by Legarreta (1985) which did not give a clear indication that the upper boundary of the diagram treated as the surface was the actual ground-surface leaving some doubt.

The validity of the proposed technique has been compared to a set of results that has been already published in a peer-reviewed journal, and the present author has applied the Carter-Tracy method for the same situation for comparison purposes. The calculated results were found to be reliable by limiting the time-step to less than 30 days which exploited the applicability of method.

Recommendations for further research

Hirschel (2007) stated that 51% of the total population of the United States, as well as 99% of the rural population, use groundwater as their source of drinking water. Now imagine the effect of groundwater contamination for a second, pretty scary isn't it? This report has proved that strong waste brine outcrops at high flows rates as shown in Figures 9, 10, and 11.

Brine outcropping issues should be prevented from arising from the first place by not commencing the injection until one of the proposed approaches has been assessed, found effective, and deployed. The solutions offered to prevent groundwater salinisation are as follows:

- Hydraulic barrier.
- An aquifer with zero thickness at some particular radius out from the wellbore.
- Bigger wellbore radius.
- Lower production rates.

An aquifer with zero thickness and a hydraulic barrier would be capable of trapping the contaminated fluid for some time but the build-up pressure as a result of trapping the fluid will be sufficient to fracture the rock leading to additional pathways for waste brine to leak back to the surface. A bigger wellbore radius will result in a decrease in pressure at wellbore but that does not mean that brine will not be leaking towards the surface.

The most feasible option found was to lower the production rate of brine, but that would result in massive financial losses. Therefore, a new idea was introduced that combined the use of a hydraulic barrier with an aquifer with zero thickness in a way that the hydraulic barrier is used to slow down the contaminated fluid enough for the aquifer with zero thickness to trap the fluid without causing the rock to fracture.

This idea might be a feasible option and could be furtherly investigated by trying to locate the optimum position for placing the hydraulic barrier close to the aquifer with zero thickness.

Acknowledgements

My Family – I just want to take the time to thank you for every little you have done for me along this road and I want to let you know that I would've never been this person without your on-going great help.

Dr Hatton – I am very grateful for patience with me, I know I did ask many questions along this road and honestly speaking you were always there to answer any question I had. I want to let you know that without your help this dissertation would have not been possible.

My brothers – I am always going to be thankful for everything that you have done for me.

Lecturers of Plymouth University – I would like to thank you all for helping me become the engineer I am now and hopefully in the very near future you are going to remember my name one day for something great.

References

Ahmed, T. (2010). Reservoir engineering handbook. Amsterdam: Gulf Professional Pub., pp.331-483.

Ahmed, M., Shayya, W., Hoey, D., Mahendran, A., Morris, R. and Al-Handaly, J. (2000). Use of evaporation ponds for brine disposal in desalination plants. Desalination, 130(2), pp.155-168.

Alghanim, J., Nashawi, I. and Malallah, A. (2012). Prediction of Water Influx of Edge-Water Drive Reservoirs Using Nonparametric Optimal Transformations. North Africa Technical Conference and Exhibition, 20-22 February, Cairo, Egypt: Society of Petroleum Engineers, pp.3-15.

Allard, D. and Chen, S. (1988). Calculation of Water Influx for Bottomwater Drive Reservoirs. SPE Reservoir Engineering, 3(02), pp.369-379.

Anderle, J., Crosby, K. and Waugh, D. (1979). Potash at Salt Springs, New Brunswick. Economic Geology, 74(2), pp.389-396.

Anderson, M. (2007). Introducing groundwater physics. Phys. Today, 60(5), pp.42-47.

Bear, J. and Verruijt, A. (1987). Modeling groundwater flow and pollution. Dordrecht: D. Reidel Pub. Co.

Bengtson, H. (2011). Darcy's Law for Modeling Groundwater Flow. [Web Page] Brighthub Engineering. Available at: http://www.brighthubengineering.com/hydraulics-civil-engineering/58490-darcys-law-for-modeling-groundwater-flow/ [Accessed 4 Apr. 2016].

Bennett, T. (2012). Transport by advection and diffusion. United States: John Wiley & Sons, pp.12-21.

Birkholzer, J., Nicot, J., Oldenburg, C., Zhou, Q., Kraemer, S. and Bandilla, K. (2013). Reply to comments by Schnaar et al. on “Brine flow up a well caused by pressure perturbation from geologic carbon sequestration: Static and dynamic evaluations” by Birkholzer et al. (2011). International Journal of Greenhouse Gas Control, 17, pp.544-545.

Carslaw, H. and Jaeger, J. (1959). Conduction of heat in solids. Oxford: Clarendon Press.

Carter, G. (2011). The Consequential Cost of Carelessness. Pollution Engineering, 43(6), pp.22-24.

Carter, R. D. and Tracy, G. W. (1960). An Improved Method for Calculating Water Influx. Society of Petroleum Engineers, AIME, 219, pp.415-417.

Charbeneau, R. (2006). Groundwater hydraulics and pollutant transport. Upper Saddle River, NJ: Waveland Press, Inc, pp.293-350.

Cookenboo, H. and Bezys, R. (2012). AMAZONAS POTASH PROPERTY TECHNICAL REPORT FOR PACIFIC POTASH CORPORATION: MIDDLE AMAZONAS BASIN, AMAZONAS STATE MINERAL CLAIMS. [Web Page] Otciq.com. Available at: https://www.otciq.com/otciq/ajax/showFinancialReportById.pdf?id=95733 [Accessed 17 Feb. 2016].

Croney, D. and Coleman, J. (1948). SOIL THERMODYNAMICS APPLIED TO THE MOVEMENT OF MOISTURE IN ROAD FOUNDATIONS. Proc. 7th Int. Congr. Appl. Mech, [online] 3, pp.163-169. Available at: https://trid.trb.org/view.aspx?id=125294.

Dake, L. (2001). The practice of reservoir engineering. Amsterdam: Elsevier, pp.108-167.

Donaldson, E., Chilingar, G. and Yen, T. (1985). Enhanced oil recovery. Amsterdam: Elsevier, pp.120-127.

Donnez, P. (2012). Essentials of reservoir engineering. Paris: Éd. Technip, pp.264-360.

Duffield, G. (2015). Glossary of Aquifer Testing Terms. [Web Page] Aqtesolv.com. Available at: http://www.aqtesolv.com/aquifer-tests/glossary-of-aquifer-testing-terms.htm#Hydraulic_Gradient [Accessed 20 Feb. 2016].

Dullien, F. (2012). Porous Media: Fluid Transport and Pore Structure. 2nd ed. San Diego: Academic Press, pp.3-17.

Ec.europa.eu. (2015). Waste statistics - Statistics Explained. [Web Page] Available at: http://ec.europa.eu/eurostat/statistics-explained/index.php/Waste_statistics [Accessed 12 Mar. 2016].

Economides, M., Economides, C., Hill, A. and Zhu, D. (2013). Petroleum production systems. 2nd ed. Upper Saddle River, NJ: Prentice Hall, pp.8-21.

Edwardson, M., Girner, H., Parkinson, H., Williams, C. and Matthews, C. (1962). Calculation of Formation Temperature Disturbances Caused by Mud Circulation. Journal of Petroleum Technology, 14(04), pp.416-426.

Ellard, O. (2015). Heat and mass transfer during the sump development in a potash solution mine. B.Eng. dissertation. Plymouth University, School of Marine Science and Engineering.

Els, F. (2013). Potash project fallout: Vale tells directors to leave Argentina over 'safety concerns' | MINING.com. [Web Page] MINING.com. Available at: http://www.mining.com/potash-project-fallout-vale-tells-directors-to-leave-argentina-over-safety-concerns-79228/ [Accessed 7 Feb 2016].

Eppelbaum, L. and Kutasov, I. (2015). Pressure and Temperature Well Testing. Boca Raton: CRC Press, pp.6-16.

Ezekwe, N. (2011). Petroleum reservoir engineering practice. Upper Saddle River, NJ: Prentice Hall, pp.295-327.

Fanchi, J. (2000). Integrated flow modeling. Amsterdam: Elsevier, pp.161-201.

Fanchi, J. (2006). Principles of applied reservoir simulation. Amsterdam: Gulf Professional Pub., pp.198-207.

Fetter, C. (2001). Applied hydrogeology. Upper Saddle River, N.J.: Prentice Hall, pp.293-296.

Garrett, D. (1996). Potash: Deposits, Processing, Properties and Uses. London: Chapman & Hall, pp.17-20.

Grove, D. (1977). The use of Galerkin finite-element methods to solve mass-transport equations. Water-Resources Investigations Report, [Web Page] p.62. Available at: https://pubs.er.gov/publication/wri779 [Accessed 11 Mar. 2015].

Hall, H. (1953). Compressibility of Reservoir Rocks. Journal of Petroleum Technology, 5(01), pp.309-331.

Haynes, W. (2015). CRC handbook of chemistry and physics, pp.969-1212.

Healy, R. and Scanlon, B. (2010). Estimating groundwater recharge. Cambridge: Cambridge University Press, pp.135-139.

Hirschel, G. (2007). The Groundwater-Stormwater Connection. Dauphin County's Stormwater Publication for Municipalities, [Web Page] 3(3), pp.1-2. Available at: http://www.dauphincd.org/articles/ywyf/ywyf3.pdf.

John, O. and Friday, U. (2011). DETERMINATION OF WATER INFLUX IN RESERVOIR IN NIGER DELTA. Wilolud Journals, 6(2), pp.37-44.

Kiernan, P. (2013). Rio Colorado potash project in Argentina. [Web Page] The Australian. Available at: http://www.theaustralian.com.au/business/mining-energy/vale-shelves-rio-colorado-potash-project-in-argentina/story-e6frg9df-1226595337879 [Accessed 16 Mar. 2016].

Kirkham, M. (2005). Principles of soil and plant water relations. Amsterdam: Elsevier Academic Press, pp.30-37.

Kresic, N. (2006). Hydrogeology and Groundwater Modeling, Second Edition. 2nd ed. Hoboken: CRC Press, pp.16-34.

Legarreta, L. (1985). Análisis estratigráfico de la formación Huitrín (cretácico inferior). Tesis Doctoral. Universidad de Buenos Aires.

Logan, B. (1999). Environmental transport processes. New York: Wiley, pp.58-63.

Masoodi, R. and Pillai, K. (2010). Darcy's law-based model for wicking in paper-like swelling porous media. AIChE Journal, 56(9), pp.2257–2262.

Menard, W. and Grove, D. (1979). A MODEL FOR CALCULATING EFFECTS OF LIQUID WASTE DISPOSAL IN DEEP SALINE AQUIFERS. [Web Page] Available at: http://pubs.usgs.gov/wri/1979/0096/report.pdf [Accessed 11 Apr. 2015].

McKinney, P. (2011). Advanced Reservoir Engineering. Gulf Professional Publishing, pp.9-37.

Myers, T. (2012). Potential Contaminant Pathways from Hydraulically Fractured Shale to Aquifers. Groundwater, 50(6), pp.872-882.

Nonner, J. (2015). Introduction to Hydrogeology, Third Edition. Introduction to Hydrogeology, Third Edit: CRC Press, pp.40-42.

Nordbotten, J. and Celia, M. (2006). Similarity solutions for fluid injection into confined aquifers. Journal of Fluid Mechanics, 561, pp.307-321.

Ong, B. (2014). The Potential Impacts of Hydraulic Fracturing on Agriculture. European Journal of Sustainable Development, 3(3), pp.63-72.

Osman, K. (2013). Soils: Principles, Properties and Management. Dordrecht: Springer, pp.67-74.

Park, Y., Sudicky, E. and Sykes, J. (2009). Effects of shield brine on the safe disposal of waste in deep geologic environments. Advances in Water Resources, 32(8), pp.1352-1358.

Pearson, S. (2013). Argentines hope Lula will pull off miracle on Vale potash mine. [Web Page] Financial Times. Available at: http://www.ft.com/cms/s/0/e30b56d4-c39d-11e2-aa5b-00144feab7de.html#axzz434kpHd4c [Accessed 14 Mar. 2016].

Philips, O. (1991) Flow and reactions in permeable rock, Cambridge University Press, Cambridge.

Phillips, O. (2009) Geological fluid dynamics, Cambridge University Press, Cambridge.

Philpotts, A. and Ague, J. (2009). Principles of igneous and metamorphic petrology. Cambridge, UK: Cambridge University Press.

Price, M. (2013). Introducing Groundwater. 2nd ed. Hoboken: Taylor and Routledge, pp.178-195.

Qanbari, F. and Clarkson, C. (2013). A new method for production data analysis of tight and shale gas reservoirs during transient linear flow period. Journal of Natural Gas Science and Engineering, 14, pp.55-65.

Qiao, X. and Li, G. (2014). FACTORS INFLUENCING THE SAFETY OF CO2 GEOLOGICAL STORAGE IN DEEP SALINE AQUIFERS. Environmental Engineering and Management Journal, 13(12), pp.2919-2920.

Réveillère, A., Rohmer, J. and Manceau, J. (2012). Hydraulic barrier design and applicability for managing the risk of CO2 leakage from deep saline aquifers. International Journal of Greenhouse Gas Control, 9, pp.62-71.

Rink, K., Kalbacher, T. and Kolditz, O. (2011). Visual data exploration for hydrological analysis. Environ Earth Sci, 65(5), pp.1395-1403.

Rojas, A. and Asociados, L. (2009). Advanced Mining Projects. [Web Page] Rojasyasociados.com. Available at: http://www.rojasyasociados.com/en/proyectos-mineros-avanzados/ [Accessed 20 Mar. 2016].

Satter, A., Iqbal, G. and Buchwalter, J. (2008). Practical enhanced reservoir engineering. Tulsa, Okla.: PennWell Corp., pp.26, 26,349.

Schreck, P. (1998). Environmental impact of uncontrolled waste disposal in mining and industrial areas in Central Germany. Environmental Geology, 35(1), pp.66-72.

Schwartz, F. and Ibaraki, M. (2011). Groundwater: A Resource in Decline. Elements, 7(3), pp.175-179.

Shankar, R. (2008). Principles of quantum mechanics. New York: Springer, pp.117-121.

Singh, A. (2015). Soil salinization and waterlogging: A threat to environment and agricultural sustainability. Ecological Indicators, 57, pp.128-130.

Slider, H. (1983). Worldwide practical petroleum reservoir engineering methods. Tulsa, Okla.: PennWell Books, pp.79-92.

Speight, J. (2014). The chemistry and technology of petroleum. Hoboken: CRC Press, Taylor and Francis, pp.55-57.

Stewart, G. (2011). Well Test Design & Analysis. Tulsa, Okla.: PennWell, pp.260-268.

Stiles, W. (1924). Permeability. London: Wheldon & Wesley.

Suckow, A. (2014). The age of groundwater – Definitions, models and why we do not need this term. Applied Geochemistry, 50, pp.222-230.

Theodore, L. (2011). Heat transfer applications for the practicing engineer. Hoboken, N.J.: Wiley, pp.25-36.

Ti, G., Ogbe, D., Munly, W. and Hatzignatiou, D. (1995). The Use of Flow Units as a Tool for Reservoir Description: A Case Study. SPE Formation Evaluation, 10(02), pp.122-128.

Tiab, D. and Donaldson, E. (2015). Petrophysics. 4th ed. Waltham: Gulf Professional Publishing, pp.67-170.

Titkov, S. (2004). Flotation of water-soluble mineral resources. International Journal of Mineral Processing, 74(1-4), pp.107-113.

Todd, D. (1959). Ground water hydrology. New York: Wiley.

Valipour, M. (2014). Future of agricultural water management in Africa. Archives of Agronomy and Soil Science, 61(7), pp.907-927.

Whitaker, S. (1986). Flow in porous media I: A theoretical derivation of Darcy's law. Transp Porous Med, 1(1), pp.3-25.

Yazicigil, H., Er, C., Ates, J. and Camur, M. (2009). Effects of solution mining on groundwater quality in the Kazan trona field, Ankara-Turkey: model predictions. Environmental Geology, 57(1), pp.157-172.

Zhang, P. (2014). Basic Hydrology - Storage Properties of Aquifers. [Web Page] mail.sci.ccny.cuny.edu. Available at: http://mail.sci.ccny.cuny.edu/~pzhang/EAS44600/EAS446lec8.pdf [Accessed 20 Feb. 2016].

Appendices for this work can be retrieved within the Supplementary Files folder which is located in the Reading Tools menu adjacent to this PDF window.